Fast Moving Target Detection in Sea Clutter Using Non-Coherent X-Band Radar

Armin Parsa
R&D Department, Rutter Inc.
St. John's, Newfoundland and Labrador, Canada

***Abstract*- The effect of antenna rotation speed on detecting a fast moving target in sea clutter using a non-coherent X-band radar is studied. The scan-to scan integration is applied using the *sigma* S6 radar processor. A helicopter (HELO) is used as a fast moving target by mimicking a landing approach to an offshore platform. The radar data was recorded using two X-band radars with horizontal polarized antennas. The two radars were installed on a mobile platform to record the data simultaneously at Cape Spear, Newfoundland. The experimental results show the performance of scan-to-scan integration process at two antenna rotation speeds for a fast moving target.**

Index Terms—Probability of detection, X-band radar, radar signal processor, sea clutter, antenna rotation speed

I. Introduction

Rutter Inc. undertook a large data collection program to record, collect, and analyze radar data of fast rescue craft (FRC), Person in Water (PIW), Helicopter (HELO) flight path approach and sea clutter at various sea states. The two main goals of this project were to enhance Rutter's understanding of the theoretical detection performance of radar when augmented with special features and to collect full bandwidth high fidelity raw radar data recordings that can be used to design and validate future product developments.

During this project two large field trials were undertaken. The first trial took place during the week of March 8th 2010 in Placentia Bay, Newfoundland at the Argentia military airbase site. During this weeklong trial, fast rescue craft (FRC) and Persons in Water (PIW) radar data was collected. The second trial took place during the months of December 2010 and January 2011 just outside of St. John's Harbor at the Skerries site, and at a second site off of Cape Spear. During this trial, FRC, PIW, helicopter (HELO) approach, and sea clutter data recordings were collected. Some of the collected data have already been analyzed for comparing the vertical and horizontal polarized radar antennas in detecting FRC and PIW [1].

This paper discusses and presents some of the results obtained from the analysis of the HELO data recorded at Cape Spear. The analysis provides performance data on the detection of helicopter as a function of range, antenna speed, and number of scans used for scan-to-scan integration (scan averaging). The probability of detection is obtained for different scenarios. Probability of detection is a standard measure that shows the radar system performance in distinguishing between the target and clutter signals [2-5].

II. Data Analysis Method

The performance of a radar system is defined by the ability of the system to differentiate the target echo signal from sea clutter and system noise. Since the target signal is mixed with noise and sea clutter, radar signal detection is probabilistic in nature. As a result, the radar performance is quantitatively defined by the Probability of Detection (P_d) and the Probability of False Alarm (P_{fa}). The probability of detecting a radar target against the background noise and clutter is called the Probability of Detection (P_d), and the probability that the reflected clutter or noise signal is mistaken as a target is called the Probability of False Alarm (P_{fa}). Calculation of the P_d and P_{fa} are therefore the main means for comparing the radar target detection performances.

In order to calculate P_d and P_{fa} from the recorded data, two zones have been set up, namely target and clutter zones. The target zone is an area containing the target and it is chosen to be as small as possible so that radar returns other than from the target are not counted as target returns. The clutter zone includes an area much bigger than the target zone. Fig. 1 shows an example of a B-scan radar image with clutter and target zones. The red circle inside the target zone indicates a target hit, and the red circles inside the clutter zone indicate clutter hits. The groups of pixels that have intensities above the threshold level and are detected as a target by Sigma S6 Radar Processor [4] are referred to as "hits". The probability of false alarm is calculated using

$$P_{fa} = \frac{\text{clutter hits - targets hits}}{\text{clutter opportunity - target opportunity}} \times 100\%. \quad (1)$$

The target and clutter opportunities are given by

$$\text{clutter opportunity} = n_c n_s \quad (2)$$

$$\text{target opportunity} = n_t n_s \quad (3)$$

where n_c and n_t are the numbers of clutter and target cells, and n_s is the number of scans used in the analysis. The number of clutter/target cells is the number of pixels inside the clutter/target zone area divided by the number of pixels inside a radar resolution cell. The radar resolution cell size is

$$\text{resolutioncell} = \frac{c\tau}{2} R\theta \quad (4)$$

where c = 3×108 m/s (speed of light), τ is the pulse length, R is the zone distance to the radar, and θ is the 3-dB antenna beamwidth.

For the P_{fa} calculated in (1), the probability of detection is obtained using

$$P_d = [\text{targethits} - (P_{fa}\, n_t n_s)] \,/\, n_s . \quad (5)$$

The precision of the P_d calculation is inversely proportional to the number of scans used in the calculations. As a rule of thumb, when the antenna rotation speed is 45 rpm, a minimum of two minutes of recording is needed to calculate the P_{fa} and P_d with sufficient precision.

For data analysis, Rutter's sigma S6 software is used. The following steps are taken to calculate P_{fa} and P_d. First, a threshold value is chosen. The threshold values are relative numbers that are set by a radar adjustment. Second, P_{fa} and P_d are calculated by counting all the clutter and target hits for all the scans. If the calculated P_{fa} is not in the desired range ($10^{-6} < P_{fa} < 10^{-4}$), the threshold is changed and the hits are counted again for all scans until the desired P_{fa} is obtained. The analysis usually requires changing the threshold and processing the data several times to obtain the desired P_{fa}.

TABLE I. SEA CONDITION DURING THE HELO TRIAL

Date	Time (GMT)	Significant Wave height (m)	Wind Speed at Shore (kn)	Sea State
Jan 25	16:30	2.4	0.9	4-5
Jan 25	17:00	2.2	0.9	4-5
Jan 25	17:30	2.2	1.7	4-5
Jan 25	18:00	NA	3.5	4-5
Jan 25	18:30	2.0	3.5	4-5

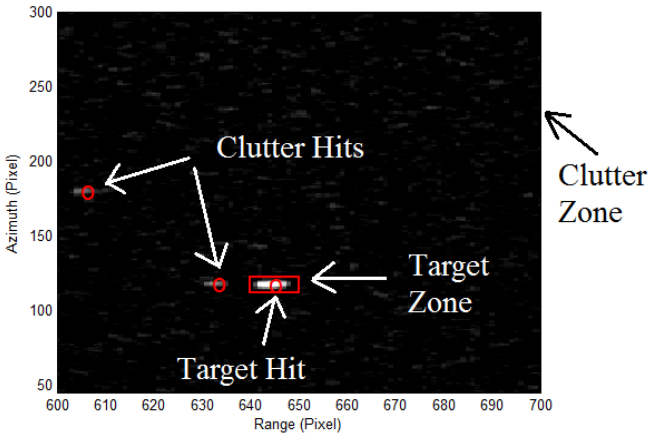

Figure 1. Clutter and target zones on a B-scan radar image. The radar image blobs are detected by the *sigma* S6 plot extractor. The blob inside the target zone is counted as a target hit, and the blobs inside the clutter zone are counted as clutter hits.

TABLE II. RADAR SYSTEMS SPECIFICATIONS

	Radar #1	**Radar #2**
Antenna Gain (dB)	31	31
Antenna Polarization	Horizontal	Horizontal
Antenna Beamwidth (degree)	0.9	0.9
Transmitter Peak Power (KW)	25	25
Operating Frequency (GHz)	9.375	9.41
Pulse Length (ns) [Short/Medium/Long]	60/250/800	50/250/750
IF Bandwidth (MHz)	20	20
Overall Noise Figure (dB) ≤	5	5
Side Lobes (dB) ≤	-35	-35
PRF (Hz) [Short/Medium/Long]	3000/1500/750	3000/1800/785
Antenna Rotation Speed (rpm)	48/60/80/120	45

III. RESULTS

The helicopter data recording was performed on January 25th, 2011. The purpose of this trial was to test the detectability of a fast target using a commercial marine navigation radar with different antenna rotation rates. A flying helicopter was chosen for this purpose which followed a flight altitude path that mimicked a helicopter landing approach to an off shore vessel. The helicopter used in this trial was Sikorsky S-92 as shown in Fig. 2(a).

Two radars (Radar #1 and Radar #2) were used during the trial, with both radars transmitting and recording simultaneously. Fig. 2(b) shows the radar van which was used during the trial. The two antennas had a beam width of 0.9 degree. Radar #1 was capable of 48, 60, 80 and 120 rpm antenna rotation rates, while the antenna of Radar #2 was only able to rotate at 28 and 45 rpm. The sea state during the trial was measured using a TRIAXYS Directional Wave Buoy (as shown in Figure 3). The wave buoy was placed off shore at Skerries, just north east of Quidi Vidi harbor (shown in Fig. 4). The wind speed during the trial was measured using a weather station (Davis Vantage Vue) close to the van. The significant wave heights obtained by the wave buoy and the radar specifications are shown in Table I and Table II, respectively.

The wave buoy at the Skerries site recorded the significant wave height for 20 minutes duration. It processed the recorded data for 10 minutes, and then transmitted the processed data to the satellite (The recorded data is shown in Table I). Since the helicopter was moving radially away from the radar, it was not possible to calculate the P_d value at a single range. Each P_d value had to be calculated over a segment of range, thereby giving an average P_d value for that segment. Table III shows the range segments that were used to analyze the data. Furthermore, it shows the helicopter altitude, the average helicopter speed, the antenna rotation speed, the radar pulse length, and the number of scans that target looks stationary (STTLS) for each range segment. The number of STTLS can be obtained using the target speed, the antenna rotation speed, and the radar pulse length. For example, a radar resolution cell at long pulse (750 ns) has a range resolution of R = 112.5 m

(Since the target is moving radially in our case, the azimuth location of the target does not change from one image to the next). When the helicopter has a speed of v = 72 knots (37 m/s), it travels one resolution cell in t = R/v=112.5/37=3.04 s. The number of collected scans per second depends on the antenna rotation speed (when the antenna speed is 45 rpm, the number of seconds per scan = 60/45 = 1.33 s). Therefore, the number of STTLS is N = 3.125/1.33 ≈ 2.3.

The P_d and P_{fa} results obtained for the two radars are shown in Table IV. The results show that the P_d is fairly low at close range, and it increases with range up to 6.9 nmi. This is due to the high amount of sea clutter which existed out to approximately 5 nmi during the trial. As a result, the average of the P_d of the two radars (with no scan averaging) is maximum when the sea clutter is completely decayed (6 nmi < range < 6.9 nmi). For the range larger than 6.9 nmi, the P_d becomes smaller due to the weaker radar return.

The results also show the effect of scan averaging on the probability of detection. In order for scan averaging to be most effective (when used on a fast moving target), the target must occupy only one radar resolution cell during the period of the scan averaging. If the target moves through more than one resolution cell, the return signal gets blurred out and the signal to noise ratio decreases.

Referring to Table IV, both radars show a similar detection performance when short pulse was used (0.1 nmi< range <7.8 nmi) and no scan averaging was applied. When scan averaging was applied, the performance of Radar #2 deteriorated significantly compared to the performance of Radar #1 since Radar #1 had a faster antenna rotation speed (which gave a larger number of STTLS).

For the case when the Long pulse was used (12.9 nmi< range <15.5 nmi), both radar antennas were rotating at 45 rpm. Referring to Table IV, it is observed that integrating (averaging) 2 scans improves the P_d significantly. Furthermore, using more scans (3 scans) for averaging does not considerably improve the detection performance (Note that the number of STTLS is 2.4 and 2.3 for Radar #1 and Radar #2, respectively).

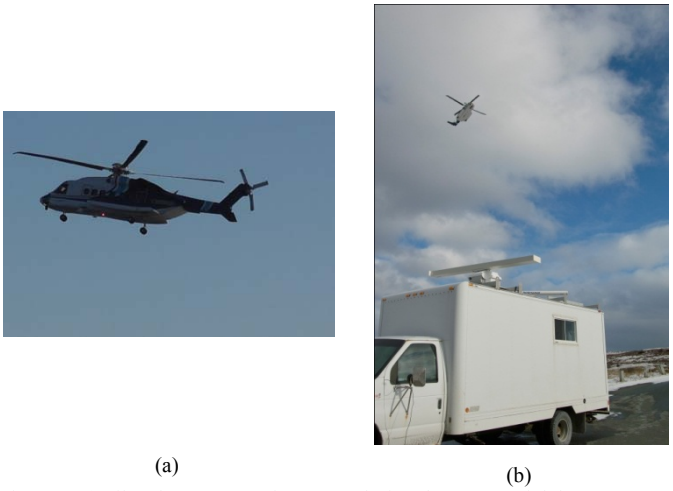

(a) (b)

Figure 2. a) Sikorsky S-92 as a fast target during the HELO trial. b) Rutter's mobile radar test platform equipped with two horizontal polarized radars during the HELO trial.

Fig. 5(a) and Fig. 5(b) show the detected target on a B-scan image after integrating (averaging) three consecutive images with antenna rotation speed of 120 rpm and 45 rpm, respectively. The target was moving with an average target speed of 75 knots (5 nmi < range < 6 nmi). Since the fast target moves more than 6 resolution cells after each scan in Fig. 5(b), the image integration (averaging) generates two extra distinct blobs in addition to the target blob on the B-scan image. Since two of the blobs are outside the target zone, they are detected as clutter. This clutter reduces the P_d value. When the antenna rotation speed is 120 rpm as shown in Fig. 5(a), the target moves approximately 2 resolution cells after each scan. The image integration generates one large blob which is detected as one target, and it remains inside the target zone. Since the target blob gets blurred out because of target movement, the signal to noise ratio decreases.

Figure 3. TRIAXYS Directional Wave Buoy used to measure the wave height.

TABLE III. HELICOPTER ALTITUDE, AVERAGE HELICOPTER SPEED, ANTENNA ROTATION SPEED, RADAR PULSE LENGTH, AND THE NUMBER OF STTLS ALONG THE FLIGHT PATH

Range (nmi)	HELO Altitude (ft)	Average HELO Speed (knot)	Antenna Rotation Speed (rpm)/ Pulse Length (ns)/ Number of STTLS	
			Radar #1	Radar #2
12.9-15.5	2000-2200	72	45/800/2.4	45/750/2.3
9.9-12	2000-2200	70	OFF	45/250/0.78
8.1-9.9	1500-2200	59	OFF	45/250/0.93
6.9-7.8	1000-1500	62	120/60/0.56	45/50/0.18
6-6.9	1000-1500	70	120/60/0.50	45/50/0.16
5-6	1000-1500	75	120/60/0.47	45/50/0.15
4-5	1000-1500	67	120/60/0.52	45/50/0.16
3-4	1000-1500	72	120/60/0.49	45/50/0.15
2-3	500-1000	62	120/60/0.56	45/50/0.18
1-2	<500	52	120/60/0.67	45/50/0.21
0.1-1	<400	51	120/60/0.69	45/50/0.21

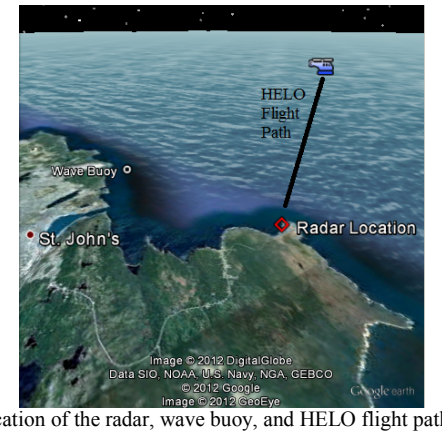

Figure 4. Location of the radar, wave buoy, and HELO flight path on the map.

TABLE IV. CALCULATED P_{fa}/P_d FOR HELO TRIAL

Range (nmi)	Pulse Length	P_{fa}/P_d HELO.3						Number of Scans Used	
		Scan Averaged = 1		Scan Averaged = 2		Scan Averaged = 3			
		Radar #1	Radar #2	Radar #1	Radar #2	Radar #1	Radar #2	Radar #1	Radar #2
12.9-15.5	L	2.4e-5/ 21%	2.4e-5/ 12%	2.1e-5/ 44%	2.2e-5/ 47%	1e-5/ 52%	8.5e-6/ 51%	107	100
9.9-12	M	OFF	1.7e-5/ 27%	OFF	1.7e-5/ 37%	OFF	2.3e-5/ 34%	NA	84
8.1-9.9	M	OFF	2.4e-5/ 62%	OFF	2.5e-5/ 81%	OFF	2.5e-5/ 83%	NA	85
6.9-7.8	S	1.6e-5/ 94%	1.1e-5/ 80%	1.2e-5/ 94%	1.9e-5/ 46%	2e-5/ 85%	1.9e-5/ 19%	103	41
6-6.9	S	1.5e-5/ 97%	2.5e-5/ 97%	1.3e-5/ 89%	2.1e-5/ 41%	1.7e-5/ 51%	1.8e-5/ 19%	92	37
5-6	S	1.8e-5/ 93%	1.9e-5/ 100%	1.7e-5/ 89%	1.9e-5/ 43%	1.6e-5/ 32%	2.4e-5/ 21%	85	35
4-5	S	2e-5/ 88%	1e-5/ 92%	1e-5/ 67%	2.1e-5/ 25%	1.3e-5/ 33%	2e-5/ 21%	88	36
3-4	S	1.1e-5/ 95%	1e-5/ 97%	1.1e-5/ 74%	1e-5/ 8%	1.2e-5/ 36%	1e-5/ 3%	96	39
2-3	S	2e-5/ 90%	2e-5/ 93%	1.7e-5/ 70%	2.2e-5/ 2%	2e-5/ 16%	3.5E-5/ 0%	110	44
1-2	S	2.2e-5/ 88%	2e-5/ 68%	1.1e-5/ 81%	2.1e-5/ 4%	1.8e-5/ 47%	2e-5/ 2%	132	53
0.1-1	S	2e-5/ 69%	1.9e-5/ 60%	1e-5/ 79%	2.3e-5/ 2%	2.1e-5/ 55%	3e-5/ 0%	126	50

IV. CONCLUSIONS

The results of the Helicopter trial show that commercial marine navigation radar may be useful for tracking a helicopter during an offshore vessel landing approach. The helicopter became detectable in the 10 to 8 Nm range and was easily detected and followed from 8 to 2 Nm. Once the helicopter entered the strong sea clutter region of the radar (0 to 2 Nm), the detectability decreased to between 60% and 88% for a moderate sea state. This is at the limit of detectability but the detectability would increase for lower sea states.

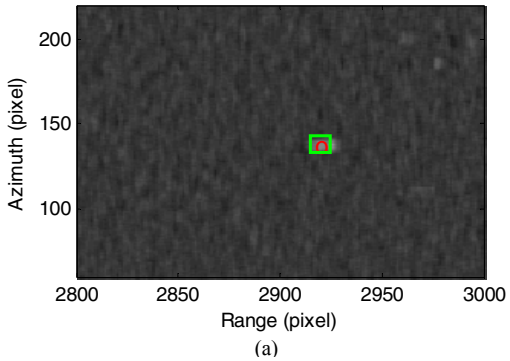

(a)

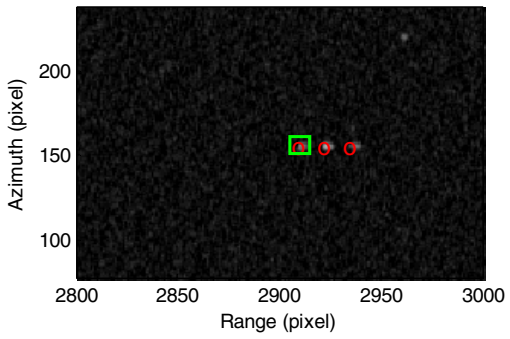

(b)

Figure 5. The detected target (red circle) is shown inside the target zone (green box) after integrating three consecutive images using, a) 120 rpm antenna rotation speed, b) 48 rpm antenna rotation speed.

When the number of scans that target looks stationary (STTLS) was above 0.8 for an aerial target, the scan-to-scan integration enhanced the detection performance. The results also revealed that increasing the antenna rotation speed improved the detection performance of a fast target in moderate sea state when integrating a fixed number of scans.

ACKNOWLEDGMENT

The author wishes to thank Sephen Hale, Desmond Smith, Tom Healy, Joe Ryan for their helpful comments, and Michael Kirby for assistance with the radar data recordings. This work was supported by RDC (Research & Development Corporation Newfoundland and Labrador) R&D Proof of Concept program.

REFERENCES

[1] A. Parsa, N. H. Hansen, "Comparison of vertically and horizontally polarized radar antennas for target detection in sea clutter – An experimental study," *in Proceedings of IEEE Radar Conference* (RADARCON), May 2012, pp. 653-658.

[2] A. Norris, "Civil marine radar," in *Radar Handbook*, MI Skolnik. Ed., 3rd ed., New York: McGraw-Hill, 2008, ch. 22.

[3] D. K. Barton, *Modern Radar System Analysis,* Norwood, MA: Artech House, 1988.

[4] G. V. Trunk, "Detection results for scanning radars employing feedback integration," *IEEE Trans. AES*, vol. 6, pp. 522-527, July 1970.

[5] K. D. Ward, C. J. Baker, S. Watts, "Maritime surveillance radar. Part 1: Radar scattering from the ocean surface," *IEE Proceedings,* vol. 137, Part F, No. 2, pp. 51-62, April. 1990.

[6] Sigma S6 Radar Processor, 2010. [online] Available: http://www.rutter.ca/sigma-s6-surveillance/